

1 **Title**

2 **Predicting sensory evaluation indices of Cheddar cheese texture by fluorescence fingerprint**  
3 **measurement coupled with an optical fiber**

4

5 **Authors**

6 Akira Chiba<sup>a, b</sup>, Mito Kokawa<sup>c,\*</sup>, Mizuki Tsuta<sup>d</sup>, Setsuko Todoriki<sup>c, d</sup>

7

8 **Affiliations and addresses**

9 <sup>a</sup> *Food Research & Development Institute, R&D Division, Morinaga Milk Industry Co., Ltd., 5-1-83*

10 *Higashihara, Zama, Kanagawa 252-8583, Japan*

11 <sup>b</sup> *Graduate School of Life and Environmental Sciences, University of Tsukuba, 1-1-1 Ten-noudai, Tsukuba,*

12 *Ibaraki 305-8577, Japan*

13 <sup>c</sup> *Faculty of Life and Environmental Sciences, University of Tsukuba, 1-1-1 Ten-noudai, Tsukuba, Ibaraki*

14 *305-8577, Japan*

15 <sup>d</sup> *Food Research Institute, National Agriculture and Food Research Organization, 2-1-12 Kan-nondai,*

16 *Tsukuba, Ibaraki 305-8642, Japan*

17

18 \*Corresponding author. Tel: +81 29 853 4659

19 *E-mail address: kokawa.mito.ke@u.tsukuba.ac.jp (M. Kokawa)*

20

21 ABSTRACT

22 A fluorescence fingerprint (FF) was used to develop a quick and non-contact practical method for  
23 predicting the sensory evaluation index of cheese texture (cheese body measurement). A partial  
24 least-squares (PLS) model was constructed from FF data and cheese body measurements of Cheddar  
25 cheeses. The cheese body measurement was successfully predicted by the PLS model with a coefficient of  
26 determination for calibration of 0.800. Notably, the reproducibility of the prediction value and the model  
27 accuracy were comparable to those of a conventional FF model despite the non-contact measurement. By  
28 exploring the variable importance in projection (VIP) and selectivity ratio (SR) of the PLS model, the  
29 fluorescence likely corresponding to oxidized lipids, Maillard reaction products, and compounds of  
30 proteins and amino acids with oxidized lipids was found to increase in intensity with the progress of  
31 ripening. This suggests that the fluorescence of these compounds contributes to the accuracy of the PLS  
32 model.

33

34

35 **1. Introduction**

36 The composition (fat, moisture, and intact casein) and maturity of natural cheese as a raw material for  
37 processed cheese has a significant impact on the product quality and stability (Guinee, Caric, & Kalab,  
38 2004; Kapoor & Metzger, 2008; Tamime, 2011). Generally, young cheese is used to produce hard  
39 processed cheese, whereas aged cheese is used to produce soft processed cheese. For example, block-type  
40 processed cheeses that are easy to slice and are elastic require a young cheese, whereas spread-type  
41 processed cheeses are primarily based on cheese with medium maturity. However, as natural cheese starts  
42 to mature immediately after manufacturing, the maturity of individual natural cheeses used to make  
43 processed cheese will differ. Therefore, to achieve products with sufficient uniformity, the blending ratio  
44 must be adjusted daily.

45 Processed cheese has numerous advantages including 1) a long shelf-life; 2) the characteristics of  
46 multiple natural cheeses through which, with additional seasoning, variations in the taste can be enhanced;  
47 3) a mild taste, making it palatable for children and people who may not be familiar with natural cheese;  
48 4) an easily modified shape and readily adjustable texture (elasticity, hardness, spreadability, and ease of  
49 slicing); and 5) high suitability for cooking (flow, ease of browning, and viscosity).

50 Assessment of the texture of cheese based on detailed measurements represents an active area of  
51 research. In particular, the relationship between physical properties and texture evaluated through  
52 instrumental measurements and sensory evaluation (Drake, Gerard, Truong, & Daubert, 1999; Foegeding,  
53 Brown, Drake, & Daubert, 2003; Guinee & Kilcawley, 2004; Lee, Imoto, & Rha, 1978; Morita et al.,  
54 2015; O'Callaghan & Guinee, 2004; Xiong, Meullenet, Hankins, & Chung, 2002) constitutes a primary  
55 area of interest. However, only a few measurement methods are actively used by processed cheese  
56 manufacturers to evaluate natural cheese as raw materials. An example of such methods currently on the  
57 market includes “Caseus Pro<sup>TM</sup>” (Gold Peg International, Inc., Braeside, Australia). This is because the

58

59 pretreatment process for evaluation and instrumental measurement is complex, the measurement results  
60 cannot be directly related to traditional sensory evaluation results, and the number of samples required for  
61 appropriate evaluation is excessively large. Therefore, in general, sensory evaluation approaches are faster.  
62 Individual processed cheese manufacturers continue to use traditional sensory evaluation or only employ  
63 instrumental measurement data directly, with each company using its own methods. For example, an index  
64 termed “cheese body measurement” is used for the sensory evaluation of physical properties. The cheese  
65 body measurement is an index of the physical maturity determined by trained experts that is based on the  
66 physical sensation of crumbling a piece of cheese between the fingers. This index varies between 1 and 10,  
67 where 10 points indicates a strong body (young texture without maturing) whereas 1 point indicates a  
68 weak body (matured texture), and is likely to vary significantly among cheese manufacturers  
69 (Mizuno & Ichihashi, 2007; Muir, 2010; Nakazawa & Hosono, 1989).

70       Alternatively, methods have been developed that utilize mid-infrared light, near-infrared light,  
71 fluorescence, and Raman spectroscopy to predict the components and physical properties of food, which  
72 are used as quick measurement methods (Nawrocka & Lamorska, 2013). As fluorescence and  
73 near-infrared spectra can be measured without sample pretreatment, these spectroscopic methods exhibit  
74 high potential for industrial use. In particular, fluorescence spectroscopy measures the emission spectrum  
75 instead of the absorption spectrum and demonstrates high sensitivity compared to that of near-infrared  
76 light (Karoui, Mazerolles, & Dufour, 2003; Kulmyrzaev, Karoui, De Baerdemaeker, & Dufour, 2007).  
77 Fluorescent compounds are sensitive to their surrounding environment (e.g., temperature, ionic  
78 concentration, pH, and polarity of solution); moreover, fluorescence spectroscopy measurements can be  
79 rapidly performed (Dufour, 2011). In addition, some investigations have been performed involving the  
80 measurement of cheese using fluorescence spectroscopy (Andersen & Mortensen, 2008; Christensen,  
81 Nørgaard, Bro, & Engelsen, 2006; Dufour, 2011; Karoui & Blecker, 2011). Furthermore, with the  
82 development of information processing technologies in recent years, fluorescence spectroscopy

83 measurements allow the rapid acquisition of emission spectra from excitation light with a continuous  
84 wavelength, such as in the form of an excitation-emission matrix (EEM), also known as a fluorescence  
85 fingerprint (FF).

86 The FF has an advantage over conventional fluorescence spectra because it includes emission spectra  
87 excited at many different excitation wavelengths. Thus, FF yields much more information as compared  
88 with the study of conventional single or double excitation wavelengths, and has the potential to estimate  
89 phenomena with high accuracy. This approach is used as a measurement method by which a large amount  
90 of information can be acquired and processed (Airado-Rodríguez, Galeano-Díaz, Durán-Merás, & Wold,  
91 2009). A FF targets not only the peak intensity of the fluorescence signal but also other wavelength ranges  
92 in which the fluorescence signal is weak. A model can then be constructed that only extracts necessary  
93 information. There are several instruments that can derive predictions based on fluorescence and a FF.  
94 Although a few analytical cases have been examined and numerous discussions have been conducted  
95 regarding the predictive accuracy obtained using these techniques, to our knowledge no reports are yet  
96 available of a detailed prediction model based on the contributing wavelength range or other factors  
97 (Lacotte et al., 2015; Liu, Sajith Babu, Coutouly, Allouche, & Amamcharla, 2016). However, there have  
98 been some cases of FFs being applied to study food (Sádecká & Tóthová, 2007) including dairy products  
99 containing cheese (Andersen & Mortensen, 2008; Boubellouta & Dufour, 2008; Christensen, Povlsen, &  
100 Sørensen, 2003).

101 Although there have been some studies that predicted cheese texture and physical properties using  
102 fluorescence spectroscopy (Garimella Purna, Prow, & Metzger, 2005; Karoui et al., 2003; Karoui &  
103 Dufour, 2006; Kulmyrzaev et al., 2005; Lebecque, Laguet, Devaux, & Dufour, 2001; Ozbekova &  
104 Kulmyrzaev, 2017), their predictions were based on the fluorescence of a limited number of entities such  
105 as tryptophan and vitamin A. Moreover, the emission spectra were measured by using only single or  
106 double excitation wavelengths, with the primary purpose being to analyze the correlation between the

107 peak intensity and components or textures. Recently, Kokawa et al. (2015) showed that a FF can predict  
108 indices of cheese maturation. They predicted the maturation time and some chemical analysis values,  
109 such as the proteolysis index (the ratio of water-soluble nitrogen content to total nitrogen content) and  
110 total free amino acid content, from FFs. They also demonstrated that the FF constitutes an effective tool  
111 for capturing changes in cheese through maturation. However, their method of measurement still requires  
112 the preparation of samples with a shape that fits the cell of the fluorescence spectrophotometer. In  
113 addition, there have been no studies where a FF has been used to predict the cheese body measurement,  
114 the index of sensory evaluation for cheese texture, for the raw materials of processed cheese.

115 In this study, our aim was to develop a rapid method for predicting the cheese body measurement  
116 using a FF, regardless of the experience level of the user. Then, we attempted to develop a method for  
117 non-contact prediction of the cheese body measurement by exploiting the optical fiber unit in a  
118 fluorescence spectrophotometer. In consideration of the practicality for industrial use, we have chosen a  
119 non-contact measurement using a fiber optics unit to eliminate the pretreatment of the sample. Although  
120 some reports are available in areas other than dairy research, no examples yet exist of application of this  
121 method to cheese texture. By removing the sample pretreatment step, measurement of the FF was easily  
122 achieved. Non-contact measurement of changes in the cheese with maturation will thus be faster than  
123 traditional methods, rendering this method useful for processed cheese manufacturers.

124

125 **2. Materials and Methods**

126 *2.1. Cheese samples*

127 Ten Australian Cheddar cheese samples were used for measurements. We performed three  
128 measurements and evaluations over time and obtained the results for a total of 30 samples. These cheese  
129 samples were matured at  $-2\text{ }^{\circ}\text{C}$ ,  $5\text{ }^{\circ}\text{C}$ ,  $10\text{ }^{\circ}\text{C}$ , and  $15\text{ }^{\circ}\text{C}$  to achieve differences in the cheese body  
130 measurement. Each cheese sample was divided into blocks for FF measurement and cheese body  
131 measurement evaluation. Cheese samples were also analyzed for moisture (ISO/IDF 4: 2004a), fat  
132 (ISO/IDF 5: 2004b), and protein (ISO/IDF 185: 2002). The pH was measured by insertion of a pH probe  
133 (D-54, Horiba, Kyoto, Japan) into the ground cheese sample.

134

135 *2.2. Evaluation of cheese body measurement*

136 The cheese body measurement was evaluated by five trained experts in consultation after adjusting  
137 the temperature of the cheese to  $5\text{ }^{\circ}\text{C}$ . The maximum score for the cheese body measurement was 10,  
138 corresponding to the strongest texture (young texture), with a score of 1 corresponding to the weakest  
139 texture (matured texture). The cheese body measurement and FF were measured on the same day or on  
140 consecutive days so that there was no difference in maturation.

141

142 *2.3. FF measurement*

143 To measure the FF of cheese, we used a fluorescence spectrophotometer (F-7000, Hitachi  
144 High-Technologies Corporation, Tokyo, Japan) and an optical fiber unit (5J0-0114-F-7000, Hitachi High-  
145 Technologies) (Mita Mala et al., 2016). The cheese samples subjected to FF measurement were adjusted  
146 to  $20\text{ }^{\circ}\text{C}$  and cut into blocks of  $3\text{ cm} \times 3\text{ cm} \times 6\text{ cm}$ . The side of the cheese samples was selected  
147 randomly and was cut immediately prior to FF measurement, and measurements were taken on a fresh  
148 surface each time. The samples were then placed on a stage with a fixed fiber unit. During measurement,

149 external light was excluded from the sample using an enclosure. The measurement conditions for the FF  
150 were an excitation wavelength of 200–500 nm, an emission wavelength of 200–800 nm, and a wavelength  
151 interval of 5 nm. The slit width of the monochromator was 10 nm for both excitation and emission  
152 wavelengths. A photomultiplier voltage of 500 V was used and the scan speed was 60,000 nm min<sup>-1</sup>. The  
153 distance between the probe tip of the fiber unit and the cheese sample was 5 mm, and the measurement  
154 was made without contact. Three replicates were measured for each cheese sample.

155

#### 156 2.4. *PLS model for prediction of cheese body measurement*

157 To predict the cheese body measurement from the FF measurements, a partial least-squares (PLS)  
158 regression model was constructed. For the multivariate analysis, MATLAB (R2016a) software  
159 (MathWorks Inc., Natick, MA, USA) and PLS Toolbox version 8.1.1 (Eigenvector Inc., Manson, WA  
160 USA) were used. FF data were preprocessed using the method of Yoshimura et al. (2014). First, as  
161 fluorescence constitutes an emission with wavelengths longer than the excitation wavelength, all data with  
162 emission wavelengths shorter than the excitation wavelengths were removed. Next, the primary light and  
163 the secondary and tertiary scattered lights, which comprise lights with the emission wavelengths at twice  
164 and three times the excitation wavelength (Fujita, Tsuta, Kokawa, & Sugiyama, 2010), respectively, were  
165 removed. Finally, excitation wavelengths shorter than 230 nm were removed because they contained  
166 significant noise. The remaining data were a combination of 3,869 excitation wavelengths and emission  
167 wavelengths.

168 In total, we performed PLS regression analysis using 90 (three replicates × 10 samples × three  
169 evaluation periods) evaluation results for FF data. The cheese body measurement was measured for 30  
170 samples (10 samples × three evaluation periods). First, the data were divided into calibration and  
171 validation sets (2:1). Specifically, the samples were aligned in order of measurement and measurements  
172 for every third sample were allocated to the validation set and those for the rest were allocated to the

173 calibration set. Next, a cross-validation model using the calibration set was employed to determine the  
174 optimum pretreatment and number of latent variables (LVs). Three preprocessing methods were used for  
175 the FF data: mean centering, normalization followed by mean centering, and autoscaling. The data were  
176 normalized so that the area underneath each spectrum was equal to 1. In autoscaling, each wavelength  
177 was scaled to 0.0 mean and unit variance. The number of LVs was determined using a PLS Toolbox  
178 algorithm that determines the descending point known as the “knee” in a scree plot (Henry, Park, &  
179 Spiegelman, 1999). Next, the selected LVs and pretreatment were used to prepare a model based on the  
180 calibration set. Furthermore, we applied this model to the validation set data to confirm the accuracy of  
181 the prediction. The accuracy of the prediction model was evaluated using the coefficients of  
182 determination of cross-validation ( $R^2_{CV}$ ) and prediction ( $R^2_P$ ) and the root-mean-square errors of cross-  
183 validation (RMSECV) and prediction (RMSEP). In addition, we calculated the variable importance in  
184 projection (VIP), the selectivity ratio (SR), and the regression vector for the model and determined the  
185 wavelength range that mainly contributes to the model.

186

187 **3. Results and Discussion**

188 *3.1. Fluorescence fingerprints and cheese compositions*

189 Figure 1 shows the mean FF for the cheese samples. An emission peak was observed in the excitation  
190 wavelength range of 290–305 nm and the emission wavelength range of 320–350 nm. This peak had a  
191 fluorescence intensity of 6131 (a.u.) and has been determined to correspond to aromatic amino acids  
192 including tryptophan (Andersen, Vishart, & Holm, 2005; Andersen & Mortensen, 2008; Mazerolles et al.,  
193 2001). In addition, the intensity was high (1201 (a.u.)) at the excitation wavelength of 320 nm and  
194 emission wavelength of 400 nm, which are likely the wavelengths of vitamin A. We focused on the peak  
195 at ex320/em400 because it has been examined in many previous reports. Fluorescence measurements for  
196 milk (Boubellouta & Dufour, 2008; Dufour & Riaublanc, 1997), soft cheese (Herbert et al., 2000),  
197 semi-hard cheese (Karoui, Dufour, & De Baerdemaeker, 2006), and processed cheese (Christensen et al.,  
198 2003) have been previously reported. The peak at the excitation wavelength of 300 nm and the emission  
199 wavelength of 680 nm represents the second-order light of the excitation wavelength of 300 nm and the  
200 emission wavelength of 335 nm, which appears owing to the light dispersion mechanism of the  
201 monochromator (i.e., the same mechanism that creates the second-order scattering light). In the FF data,  
202 similar peaks were detected to those in Kokawa et al. (2015); thus, we confirmed that a non-contact FF  
203 could be obtained for cheese using an optical fiber.

204 Table 1 shows the age, composition and pH of 10 sample cheeses. It was confirmed that there was  
205 little difference in composition and pH between samples.

206

207 *3.2. PLS prediction model*

208 Table 2 shows the LVs and prediction accuracy of the PLS regression model for each pretreatment.

209 Before performing the PLS regression analysis, four pretreatments were evaluated to optimize the model  
210 in terms of  $R^2CV$  and  $RMSECV$ . The present model that used the mean center and normalization followed

211 by the mean center as a pretreatment exhibited a similar level of accuracy with  $R^2CV$  of 0.787 and  
212 RMSECV of 0.456. “Normalize” constitutes the pretreatment whereby the sum of the luminance is  
213 normalized to be 1. This pretreatment can reduce the variation caused by differences in overall brightness  
214 (although the spectral shapes are the same). In this study, it made no difference in precision whether  
215 “normalize” was performed or not; there is thus a possibility that such variation was small. The  
216 “autoscale” and “normalize + autoscale” were not adopted because the precision was low.

217 Figure 2 (the calibration set) and Fig. 3 (the validation set) show the relationship between the cheese  
218 body measurement predicted from the FF using the optical fiber unit and the actually evaluated cheese  
219 body measurement. The prediction model was developed with three LVs using the pretreatment of the  
220 mean center. In the validation set, we obtained a strong correlation ( $R^2P = 0.826$ ) and small prediction  
221 error (RMSEP = 0.436). Additionally, the relative standard deviation (RSD) of the body value predicted  
222 by FFs in the three replicates was 0.21% minimum and 5.4% maximum. The average of RSD with three  
223 replicates in all 30 samples was 1.6%. These values show that this method can be applied repeatedly with  
224 just 1–2% variation and has high reproducibility. The results shown in Figs. 2 and 3 indicate that 1) the  
225 FF can predict the cheese body measurement although attention is required for cheese body  
226 measurements of around six, and 2) using the optical fiber unit, the cheese body measurement can be  
227 predicted through non-contact measurement.

228 The evaluation of cheese body measurements by the experts in this study often resulted in cheese  
229 body measurements of around six; thus, the distribution of the evaluation data was unequal. This is likely  
230 to have reduced the prediction accuracy. As the predicted cheese body measurements of around six have a  
231 higher variation than that of other cheese body measurements, the handling of results close to this value  
232 requires attention. To further improve the accuracy, the number of samples can be increased, or samples  
233 should be selected so that the distribution of cheese body measurements across the scoring range is even.  
234

235 3.3. *VIP and SR scores of the PLSR model plotted using FF contour representation*

236 Figure 4 shows the VIP and SR scores as a contour map to identify the range of wavelengths that  
237 contributes to the PLS regression model. Two wavelength ranges with high VIP scores were identified  
238 (Fig. 4a). Wavelengths with VIP scores of 1 or higher are known to be important variables in the model  
239 (Mehmood, Liland, Snipen, & Sæbø, 2012). The highest VIP score (69.9) was observed in the wavelength  
240 ranges with an excitation wavelength of 305 nm and an emission wavelength of 340 nm. Subsequently,  
241 the wavelength ranges with an excitation wavelength of 340 nm and an emission wavelength of 400 nm  
242 also showed high VIP value (VIP score = 15.9). The VIP value of the wavelength ranges with an  
243 excitation wavelength of 300 nm and an emission wavelength of 680 nm was also high, but we did not  
244 pursue this range because it represented the second-order light of an excitation wavelength of 300 nm and  
245 an emission wavelength of 340 nm. As has been previously reported, the excitation wavelength of 305 nm  
246 and emission wavelength of 340 nm were considered to represent tryptophan and aromatic amino acids  
247 (Andersen et al., 2005; Andersen & Mortensen, 2008; Mazerolles et al., 2001).

248 As an alternative, Fig. 4b shows a contour map of the SR scores. SR scores provide a numerical  
249 evaluation of the utility of each variable in a regression model. The SR scores can be used to build a  
250 model with even higher accuracy by excluding wavelength ranges with low SR scores and selecting  
251 wavelengths with only high SR scores (Rajalahti et al., 2009). In the present study, we used the F-test  
252 (95%) standard to select wavelength ranges with a large contribution (Farrés, Platikanov, Tsakovski, &  
253 Tauler, 2015). The SR score of the F-test (95%) was 1.55. Wavelength ranges with a SR score above this  
254 value (SR score > 1.55) included the excitation wavelengths of 335–445 nm and emission wavelengths of  
255 370–520 nm. In these ranges, the excitation wavelength of 385 nm and emission wavelength of 460 nm  
256 comprised the peak wavelengths. The peak SR score for these excitation-emission wavelengths was 7.11.  
257 The SR score of the excitation wavelength of 350 nm and the emission wavelength of 770 nm was also  
258 high, but this wavelength range was also not further pursued because it represented second-order light of

259 the excitation wavelength of 340 nm and the emission wavelength of 400 nm.

260 As VIP scores only take positive values, we used the regression coefficient (regression vector) shown  
261 in Fig. 4c to determine whether the wavelengths correlated positively or negatively with the cheese body  
262 measurements. The regression vector for each VIP peak revealed that the value was positive at the  
263 excitation wavelength of 305 nm and emission wavelength of 340 nm and negative at the excitation  
264 wavelength of 340 nm and emission wavelength of 400 nm. This suggests that the fluorescence intensity  
265 of the former wavelengths decreases as the cheese body measurement decreases, whereas that of the latter  
266 wavelengths increases.

267 Figure 5a shows the emission spectra of all samples at an excitation wavelength of 340 nm. The peak  
268 intensity around the emission wavelength of 400 nm increased as the cheese body measurement  
269 decreased; the correlation coefficient of the fluorescence at the excitation wavelength of 340 nm and  
270 emission wavelength of 400 nm with the cheese body measurement was  $-0.77$ . The fluorescence intensity  
271 of each fluorophore reflects how they are metabolized during cheese maturation. In this study, we  
272 considered that the wavelength range of excitation wavelength of 340 nm and emission wavelength of 400  
273 nm, which exhibited high correlation with cheese body measurement, was related to substances that  
274 increased during cheese maturation.

275 Numerous investigations have focused on the range near the excitation wavelength of 340 nm and the  
276 emission wavelength of 400 nm. Stapelfeldt & Skibsted (1994) reported that in a model system of dairy  
277 products and  $\beta$ -lactoglobulin, accumulated secondary lipid oxidation products emit fluorescence at  
278 excitation wavelengths of 350 nm and emission wavelength of 410 nm. Morales, Romero, &  
279 Jiménez-Pérez (1996) monitored the fluorescence of Maillard reaction products during the thermal  
280 processing of a model system using milk and dairy products at an excitation wavelength of 347 nm and  
281 emission wavelength of 415 nm. These model system studies demonstrated that oxidized lipid and  
282 Maillard reaction products of milk and dairy products could be monitored via their fluorescence in the

283 range near the excitation wavelength of 340 nm and the emission wavelength of 400 nm. In addition,  
284 Kokawa et al. (2015) selected peaks at an excitation wavelength of 345 nm and emission wavelength of  
285 400 nm as the wavelength values with a large contribution to the PLS regression model in the FF of  
286 cheese maturation indices, which suggested that oxidized lipids and Maillard reaction products are  
287 present in Cheddar cheese. These are thus considered to be the same substances as measured in the  
288 present study, as we also focused on these wavelengths based on the VIP values in this study. Notably,  
289 although Maillard reactions do not proceed actively in hard and semi hard cheeses, studies using  
290 Manchego (Corzo, Villamiel, Arias, Jiménez-Pérez, & Morales, 2000), Cheddar, Gouda and Emmental  
291 (Schwietzke, Schwarzenbolz, & Henle, 2009), Harzer and Gouda cheeses (Spanneberg, Salzwedel, &  
292 Glomb, 2012) have been reported that the Maillard reaction proceeded along with cheese maturation of  
293 these cheeses. These studies measured Maillard reaction products in young and matured cheese using  
294 high performance liquid chromatography analysis. As the amount of Maillard reaction products tends to  
295 increase during cheese maturation, they are likely to show correlation with the cheese body measurement.

296 Figure 5b shows the emission spectra at an excitation wavelength of 385 nm, where the SR score was  
297 the highest. The maximum wavelength of the fluorescence was between 500 and 550 nm, although  
298 multiple peaks were also confirmed around 460 nm. The fluorescence peaks around 460 nm increased in  
299 intensity as the cheese body measurement decreased, with the correlation coefficient between the cheese  
300 body measurement and the fluorescence intensity at an excitation wavelength of 385 nm and emission  
301 wavelength of 460 nm being  $-0.79$ .

302 The fluorescence constituents most commonly reported in this range are the reaction products  
303 between amino acids, proteins, and oxidized lipids. Kikugawa, Takayanagi, & Watanabe (1985) reported  
304 that the reaction product of malondialdehyde (MDA) and lysine monomer generated by lipid oxidation  
305 has a maximum excitation wavelength of 395 nm and maximum emission wavelength of 466–470 nm. In  
306 addition, they reported that the reaction product of MDA and a model protein, polylysine, has a maximum

307 excitation wavelength of 398 nm and maximum emission wavelength of 470 nm. The same group  
308 (Kikugawa & Beppu, 1987) reported that with the generation of fluorescent substances through lipid  
309 oxidation in tissues and cells, the reaction of MDA and primary amines in the presence of monofunctional  
310 aldehydes is promoted, generating fluorescent 1,4-disubstituted 1,4-dihydropyridine-3,5-dicarbaldehydes.  
311 The maximum excitation wavelength of the reaction products was 386–403 nm and maximum emission  
312 wavelength was 444–465 nm. Yamaki, Kato, & Kikugawa (1992) reported that the reaction product of  
313 hexenal and glycine ethyl had a maximum excitation wavelength of 392 nm and maximum emission  
314 wavelength of 455 nm. Veberg, Vogt, & Wold (2006) fixed the excitation wavelength at 382 nm and  
315 reported the fluorescence of the reaction product of oxidized lipids (aldehydes) and amino acids. They  
316 found that the reaction product of lysine and 2-hexenal has a maximum fluorescence at 471 nm, whereas  
317 the reaction product of lysine and 2,4-heptadienal has a maximum fluorescence at 472 nm. The reaction  
318 product of malondialdehyde and glycine shows maximum fluorescence at 465–469 nm, whereas the  
319 reaction with lysine shows maximum fluorescence at 467–469 nm (both with an excitation wavelength of  
320 382 nm). Furthermore, they showed that the fluorescence is generated at a temperature of 4 °C under  
321 refrigeration. The same group (Veberg, Olsen, Nilsen, & Wold, 2007) also reported that the maximum  
322 emission wavelength for oxidized lipids in butter during light irradiation was 465–470 nm, and indicated  
323 that the peak emission of the oxidized lipids occurs around 470 nm regardless of the type of food (e.g.,  
324 salted cod, turkey, chicken meat, or salmon pâté). In the present experiment, we did not use any  
325 irradiation during storage; however, oxidized lipids may be generated during long-term storage.

326 In comparison, lumichrome, generated by the photo-oxidation of riboflavin, has an  
327 excitation-emission peak near the same range; however, the peak wavelengths were an excitation  
328 wavelength of 360 nm and emission wavelength of 450 nm in the model system (Fox & Thayer, 1998) but  
329 an excitation wavelength of 370 nm and emission wavelength of 430 nm in yogurt (Christensen, Becker,  
330 & Frederiksen, 2005). In addition to this discrepancy, the low contribution of riboflavin fluorescence to

331 the model also suggests that the effect of lumichrome was small. If lumichrome had high relevance with  
332 the accuracy of the PLS model, riboflavin should also show high relevance. However, the wavelength  
333 area corresponding to riboflavin fluorescence did not show high contribution to the PLS regression  
334 model.

335 Figure 5c shows the emission spectra at an excitation wavelength of 305 nm, at which there is a peak  
336 in VIP. Peaks near the emission wavelength of 340 nm showed high fluorescence intensity; however, the  
337 correlation with the cheese body measurement was low, with the correlation coefficient of the  
338 fluorescence intensity with the cheese body measurement at an excitation wavelength of 305 nm and  
339 emission wavelength of 340 nm being 0.05. Although tryptophan and aromatic amino acids represented  
340 by these peak wavelengths have been used to predict the parameters of dairy products including cheese  
341 (Andersen & Mortensen, 2008), in the present study, the correlation coefficient was low and the  
342 contribution to the PLS regression model was low. This wavelength range has strong fluorescence  
343 intensity and captures changes well, but by performing a comprehensive analysis such as on the FF,  
344 changes during cheese maturation will have even higher correlation, which will allow the identification of  
345 the range of wavelengths contributing to the accuracy of the PLS regression model. We also suggest that  
346 in future studies, it should be possible to confirm the substances showing high correlation with the  
347 changes in the cheese body measurement by performing chemical analysis (e.g., extraction and high  
348 performance liquid chromatography) to quantify the substances, and then comparing the relative quantity  
349 of the substance of interest with the cheese body measurement.

350

#### 351 **4. Conclusion**

352 We showed that non-contact FF measurements using an optical fiber probe can be used to predict the  
353 cheese body measurement of Cheddar cheese. Compared with conventional fluorescence measurements  
354 in a photometer chamber using cells to hold the sample, it was possible to develop a more practical

355 method. The predictive ability of the model was reliable with a strong correlation ( $R^2P = 0.826$ ) and small  
356 prediction error ( $RMSEP = 0.436$ ). Moreover, the average RSD of the three replicates in all 30 samples  
357 was 1.6%. These values show that this method can be applied repeatedly with only 1–2% variation and has  
358 high reproducibility. Despite the non-contact FF measurement, it was confirmed that the accuracy of this  
359 prediction model is equivalent to that of previous studies. However, as the predicted values for cheese  
360 body measurements of around six show large variation, it is necessary to improve the accuracy by using  
361 data that reflect a more uniform distribution of cheese body measurements.

362 The wavelength ranges of oxidized lipids and Maillard reaction products (excitation wavelength of  
363 340 nm and emission wavelength of 400 nm), which were assumed to make a large contribution to the  
364 prediction of indices of cheese maturation (maturation time, proteolysis index, and free amino acid  
365 content) in previous reports, were shown to also make a large contribution to the present cheese body  
366 measurement prediction model.

367 By exploring the SR scores, we discovered a new wavelength range with a large contribution to the  
368 PLS regression model. These wavelengths were considered to correspond to oxidized lipids or to  
369 compounds of proteins and amino acids with oxidized lipids. Additional studies are necessary to confirm  
370 whether these products are responsible for these new wavelength changes, such as by comparing the  
371 results of quantification of these product contents with the FF measurements. Thus, our results suggest that  
372 the rapid and simple non-contact FF method developed herein for predicting the cheese body measurement  
373 may be suitable for industrial application to enhance the quality and reliability of processed cheese  
374 production.

375

376 Funding: This research did not receive any specific grant from funding agencies in the public, commercial,  
377 or not-for-profit sectors.

378

379 **References**

380

381 Airado-Rodríguez, D., Galeano-Díaz, T., Durán-Merás, I., & Wold, J. P. (2009). Usefulness of  
382 fluorescence excitation-emission matrices in combination with PARAFAC, as fingerprints of red  
383 wines. *Journal of Agricultural and Food Chemistry*, 57, 1711-1720.

384 Andersen, C. M., & Mortensen, G. (2008). Fluorescence spectroscopy: a rapid tool for analyzing dairy  
385 products. *Journal of Agricultural and Food Chemistry*, 56, 720-729.

386 Andersen, C. M., Vishart, M., & Holm, V. K. (2005). Application of fluorescence spectroscopy in the  
387 evaluation of light-induced oxidation in cheese. *Journal of Agricultural and Food Chemistry*, 53,  
388 9985-9992.

389 Boubellouta, T., & Dufour, E. (2008). Effects of mild heating and acidification on the molecular structure  
390 of milk components as investigated by synchronous front-face fluorescence spectroscopy  
391 coupled with parallel factor analysis. *Applied Spectroscopy*, 62, 490-496.

392 Christensen, J., Becker, E. M., & Frederiksen, C. S. (2005). Fluorescence spectroscopy and PARAFAC in  
393 the analysis of yogurt. *Chemometrics and Intelligent Laboratory Systems*, 75, 201-208.

394 Christensen, J., Nørgaard, L., Bro, R., & Engelsen, S. B. (2006). Multivariate autofluorescence of intact  
395 food systems. *Chemical Reviews*, 106, 1979-1994.

396 Christensen, J., Povlsen, V. T., & Sørensen, J. (2003). Application of fluorescence spectroscopy and  
397 chemometrics in the evaluation of processed cheese during storage. *Journal of Dairy Science*, 86,  
398 1101-1107.

399 Corzo, N., Villamiel, M., Arias, M., Jiménez-Pérez, S., & Morales, F. J. (2000). The Maillard reaction  
400 during the ripening of Manchego cheese. *Food Chemistry*, 71, 255-258.

401 Drake, M. A., Gerard, P. D., Truong, V. D., & Daubert, C. R. (1999). Relationship between instrumental  
402 and sensory measurements of cheese texture. *Journal of Texture Studies*, 30, 451-476.

403 Dufour, E. (2011). Recent advances in the analysis of dairy product quality using methods based on the  
404 interactions of light with matter. *International Journal of Dairy Technology*, 64, 153-165.

405 Dufour, E., & Riaublanc, A. (1997). Potentiality of spectroscopic methods for the characterisation of dairy  
406 products. i. front-face fluorescence study of raw, heated and homogenised milks. *Le Lait*, 77,  
407 657-670.

408 Farrés, M., Platikanov, S., Tsakovski, S., & Tauler, R. (2015). Comparison of the variable importance in  
409 projection (VIP) and of the selectivity ratio (SR) methods for variable selection and  
410 interpretation. *Journal of Chemometrics*, 29, 528-536.

411 Foegeding, E. A., Brown, J., Drake, M., & Daubert, C. R. (2003). Sensory and mechanical aspects of  
412 cheese texture. *International Dairy Journal*, 13, 585-591.

413 Fox, J. B. Jr., & Thayer, D. W. (1998). Radical oxidation of riboflavin. *International Journal for Vitamin  
414 and Nutrition Research*, 68, 174-180.

415 Fujita, K., Tsuta, M., Kokawa, M., & Sugiyama, J. (2010). Detection of deoxynivalenol using  
416 fluorescence excitation-emission matrix. *Food and Bioprocess Technology*, 3, 922-927.

417 Garimella Purna, S. K., Prow, L. A., & Metzger, L. E. (2005). Utilization of front-face fluorescence  
418 spectroscopy for analysis of process cheese functionality. *Journal of Dairy Science*, 88, 470-477.

419 Guinee, T. P., Caric, M., & Kalab, M. (2004). Pasteurized processed cheese and substitute/imitation  
420 cheese products. *Cheese: Chemistry, Physics and Microbiology*, 2, 349-394.

421 Guinee, T. P., & Kilcawley, K. N. (2004). Cheese as an ingredient. *Cheese: Chemistry, Physics and  
422 Microbiology* 2, 395-428.

423 Henry, R. C., Park, E. S., & Spiegelman, C. H. (1999). Comparing a new algorithm with the classic  
424 methods for estimating the number of factors. *Chemometrics and Intelligent Laboratory Systems*,  
425 48, 91-97.

426 Herbert, S., Riou, N. M., Devaux, M. F., Riaublanc, A., Bouchet, B., Gallant, D. J., et al. (2000).

427 Monitoring the identity and the structure of soft cheeses by fluorescence spectroscopy. *Le Lait*,  
428 80, 621-634.

429 ISO/IDF. (2002). *Milk and milk products: Determination of nitrogen content: Routine method using*  
430 *combustion according to the Dumas principle. 185:2002*. Brussels, Belgium: International Dairy  
431 Federation.

432 ISO/IDF. (2004a). *Cheese and processed cheese: Determination of the total solids content (Reference*  
433 *method). 4:2004*. Brussels, Belgium: International Dairy Federation.

434 ISO/IDF. (2004b). *Cheese and processed cheese products: Determination of fat content: Gravimetric*  
435 *method (Reference method). 5:2004*. Brussels, Belgium: International Dairy Federation.

436 Kapoor, R., & Metzger, L. E. (2008). Process cheese: scientific and technological aspects - a review.  
437 *Comprehensive Reviews in Food Science and Food Safety*, 7, 194-214.

438 Karoui, R., & Blecker, C. (2011). Fluorescence spectroscopy measurement for quality assessment of food  
439 systems - a review. *Food and Bioprocess Technology*, 4, 364-386.

440 Karoui, R., & Dufour, E. (2006). Prediction of the rheology parameters of ripened semi-hard cheeses  
441 using fluorescence spectra in the UV and visible ranges recorded at a young stage. *International*  
442 *Dairy Journal*, 16, 1490-1497.

443 Karoui, R., Dufour, E., & De Baerdemaeker, J. (2006). Common components and specific weights  
444 analysis: a tool for monitoring the molecular structure of semi-hard cheese throughout ripening.  
445 *Analytica Chimica Acta*, 572, 125-133.

446 Karoui, R., Mazerolles, G., & Dufour, E. (2003). Spectroscopic techniques coupled with chemometric  
447 tools for structure and texture determinations in dairy products. *International Dairy Journal*, 13,  
448 607-620.

449 Kikugawa, K., & Beppu, M. (1987). Involvement of lipid oxidation products in the formation of  
450 fluorescent and cross-linked proteins. *Chemistry and Physics of Lipids*, 44, 277-296.

451 Kikugawa, K., Takayanagi, K., & Watanabe, S. (1985). Polylysines modified with malonaldehyde,  
452 hydroperoxylinoleic acid and monofunctional aldehydes. *Chemical & Pharmaceutical Bulletin*,  
453 33, 5437-5444.

454 Kokawa, M., Ikegami, S., Chiba, A., Koishihara, H., Trivittayasil, V., Tsuta, M., et al. (2015). Measuring  
455 cheese maturation with the fluorescence fingerprint. *Food Science and Technology Research*, 21,  
456 549-555.

457 Kulmyrzaev, A., Dufour, E., Noël, Y., Hanafi, M., Karoui, R., Qannari, E. M., et al. (2005). Investigation  
458 at the molecular level of soft cheese quality and ripening by infrared and fluorescence  
459 spectroscopies and chemometrics - relationships with rheology properties. *International Dairy*  
460 *Journal*, 15, 669-678.

461 Kulmyrzaev, A. A., Karoui, R., De Baerdemaeker, J., & Dufour, E. (2007). Infrared and fluorescence  
462 spectroscopic techniques for the determination of nutritional constituents in foods. *International*  
463 *Journal of Food Properties*, 10, 299-320.

464 Lacotte, P., Gomez, F., Bardeau, F., Muller, S., Acharid, A., Quervel, X., et al. (2015). Amaltheys: A  
465 fluorescence-based analyzer to assess cheese milk denatured whey proteins. *Journal of Dairy*  
466 *Science*, 98, 6668-6677.

467 Lebecque, A., Laguët, A., Devaux, M. F., & Dufour, É. (2001). Delineation of the texture of salers cheese  
468 by sensory analysis and physical methods. *Le Lait*, 81, 609-624.

469 Lee, C.H., Imoto, E.M., & Rha, C. (1978). Evaluation of cheese texture. *Journal of Food Science*, 43,  
470 1600-1605.

471 Liu, Z., Sajith Babu, K., Coutouly, A., Allouche, F., & Amamcharla, J. K. (2016). Prediction of intact  
472 casein in cheese by using Amaltheys: a front-face fluorescence analyzer. *Journal of Animal*  
473 *Science*, 94, 250.

474 Mazerolles, G., Devaux, M. F., Duboz, G., Duployer, M. H., Riou, N. M., & Dufour, E. (2001). Infrared

475 and fluorescence spectroscopy for monitoring protein structure and interaction changes during  
476 cheese ripening. *Le Lait*, 81, 509-527.

477 Mehmood, T., Liland, K. H., Snipen, L., & Sæbø, S. (2012). A review of variable selection methods in  
478 partial least squares regression. *Chemometrics and Intelligent Laboratory Systems*, 118, 62-69.

479 Mita Mala, D., Yoshimura, M., Kawasaki, S., Tsuta, M., Kokawa, M., Trivittayasil, V., et al. (2016). Fiber  
480 optics fluorescence fingerprint measurement for aerobic plate count prediction on sliced beef  
481 surface. *LWT - Food Science and Technology*, 68, 14-20.

482 Mizuno, R., & Ichihashi, N. (2007). Characterization of two types of cheddar cheese as ingredients for  
483 processed cheese. *Nippon Shokuhin Kagaku Kogaku Kaishi*, 54, 395-400.

484 Morales, F. J., Romero, C., & Jiménez-Pérez, S. (1996). Fluorescence associated with Maillard reaction in  
485 milk and milk-resembling systems. *Food Chemistry*, 57, 423-428.

486 Morita, A., Araki, T., Ikegami, S., Okaue, M., Sumi, M., Ueda, R., et al. (2015). Coupled stepwise  
487 PLS-VIP and ANN modeling for identifying and ranking aroma components contributing to the  
488 palatability of cheddar cheese. *Food Science and Technology Research*, 21, 175-186.

489 Muir, D. D. (2010). The grading and sensory profiling of cheese. In B. A. Law, A. Y. Tamime (Eds.).  
490 *Technology of Cheesemaking* (pp. 440-474): Wiley-Blackwell.

491 Nakazawa, Y., & Hosono, A. (1989). *Recent advances in cheese science and technology*. New Food  
492 Industry.

493 Nawrocka, A., & Lamorska, J. (2013). Determination of food quality by using spectroscopic methods. In  
494 S. Grundas & A. Stepniewski (Eds.), *Advances in Agrophysical Research* (Ch. 14). InTech.

495 O'Callaghan, D. J., & Guinee, T. P. (2004). Rheology and texture of cheese. In P. F. Fox, P. L. H.  
496 McSweeney, T. M. Cogan & T. P. Guinee (Eds.), *Cheese: Chemistry, Physics and Microbiology*  
497 (Vol. 1, pp. 511-540). London: Academic Press.

498 Ozbekova, Z., & Kulmyrzaev, A. (2017). Fluorescence spectroscopy as a non destructive method to

499 predict rheological characteristics of tilsit cheese. *Journal of Food Engineering*, 210, 42-49.

500 Rajalahti, T., Arneberg, R., Berven, F. S., Myhr, K. M., Ulvik, R. J., & Kvalheim, O. M. (2009).

501 Biomarker discovery in mass spectral profiles by means of selectivity ratio plot. *Chemometrics*

502 *and Intelligent Laboratory Systems*, 95, 35-48.

503 Sádecká, J., & Tóthová, J. (2007). Fluorescence spectroscopy and chemometrics in the food classification

504 - a review. *Czech Journal of Food Sciences*, 25, 159-173.

505 Schwietzke, U., Schwarzenbolz, U., & Henle, T. (2009). Influence of cheese type and maturation time on

506 the early Maillard reaction in cheese. *Czech Journal of Food Sciences*, 27, S140-S142.

507 Spanneberg, R., Salzwedel, G., & Glomb, M. A. (2012). Formation of early and advanced Maillard

508 reaction products correlates to the ripening of cheese. *Journal of Agricultural and Food*

509 *Chemistry*, 60, 600-607.

510 Stapelfeldt, H., & Skibsted, L. H. (1994). Modification of  $\beta$ -lactoglobulin by aliphatic aldehydes in

511 aqueous solution. *Journal of Dairy Research*, 61, 209-219.

512 Tamime, A. Y. (2011). *Processed cheese and analogues* (Vol. 16). John Wiley & Sons.

513 Veberg, A., Olsen, E., Nilsen, A. N., & Wold, J. P. (2007). Front-face fluorescence measurement of

514 photosensitizers and lipid oxidation products during the photooxidation of butter. *Journal of*

515 *Dairy Science*, 90, 2189-2199.

516 Veberg, A., Vogt, G., & Wold, J. P. (2006). Fluorescence in aldehyde model systems related to lipid

517 oxidation. *LWT - Food Science and Technology*, 39, 562-570.

518 Xiong, R., Meullenet, J. F., Hankins, J. A., & Chung, W. K. (2002). Relationship between sensory and

519 instrumental hardness of commercial cheeses. *Journal of Food Science*, 67, 877-883.

520 Yamaki, S., Kato, T., & Kikugawa, K. (1992). Characteristics of fluorescence formed by the reaction of

521 proteins with unsaturated aldehydes, possible degradation products of lipid radicals. *Chemical*

522 *and Pharmaceutical Bulletin*, 40, 2138-2142.

523 Yoshimura, M., Sugiyama, J., Tsuta, M., Fujita, K., Shibata, M., Kokawa, M., et al. (2014). Prediction of  
524 aerobic plate count on beef surface using fluorescence fingerprint. *Food and Bioprocess*  
525 *Technology*, 7, 1496-1504.  
526

527 **Figure legends**

528

529 **Fig. 1.** Examples of fluorescence fingerprints (FFs) of Cheddar cheese surfaces obtained using optical  
530 fiber in the range of normal intensities (0–6000 intensity (a.u.)).

531

532 **Fig. 2.** Predicted vs measured cheese body measurements obtained by PLSR calibration. Bold lines show  
533  $y = x$ .

534

535 **Fig. 3.** Predicted vs measured cheese body measurements obtained by PLSR validation. Bold lines show  
536  $y = x$ .

537

538 **Fig. 4.** Contour plot of each score in the PLS model: (a) VIP, (b) SR, (c) regression vector.

539

540 **Fig. 5.** Fluorescence emission spectra color-coded by cheese body measurement at excitation wavelengths  
541 of (a) 340 nm, (b) 385 nm, and (c) 305 nm.

**Table 1**

Physico-chemical compositions of the 10 Cheddar cheeses.

Cheese samples	Age at measurements (days)			Storage temperature (°C)	pH	Dry matter (g/100g <sup>-1</sup> )	Fat (g/100g <sup>-1</sup> )	Protein (g/100g <sup>-1</sup> )	Salt (g/100g <sup>-1</sup> )
	1st	2nd	3rd						
1	231	269	318	-2	5.42	67.4	34.9	27.5	1.9
2	132	170	219	-2	5.40	67.3	34.7	27.4	2.0
3	111	149	198	-2	5.47	67.6	34.6	27.5	2.1
4	231	269	318	5	5.48	67.7	34.9	27.3	1.9
5	132	170	219	5	5.43	67.9	35.3	27.7	2.2
6	231	269	318	10	5.39	67.7	35.5	27.2	1.9
7	203	241	290	10	5.52	67.6	35.5	27.4	1.9
8	231	269	318	15	5.55	68.1	35.6	27.2	2.1
9	203	241	290	15	5.47	68.0	35.1	27.7	2.1
10	132	170	219	15	5.41	67.6	35.3	27.5	2.1

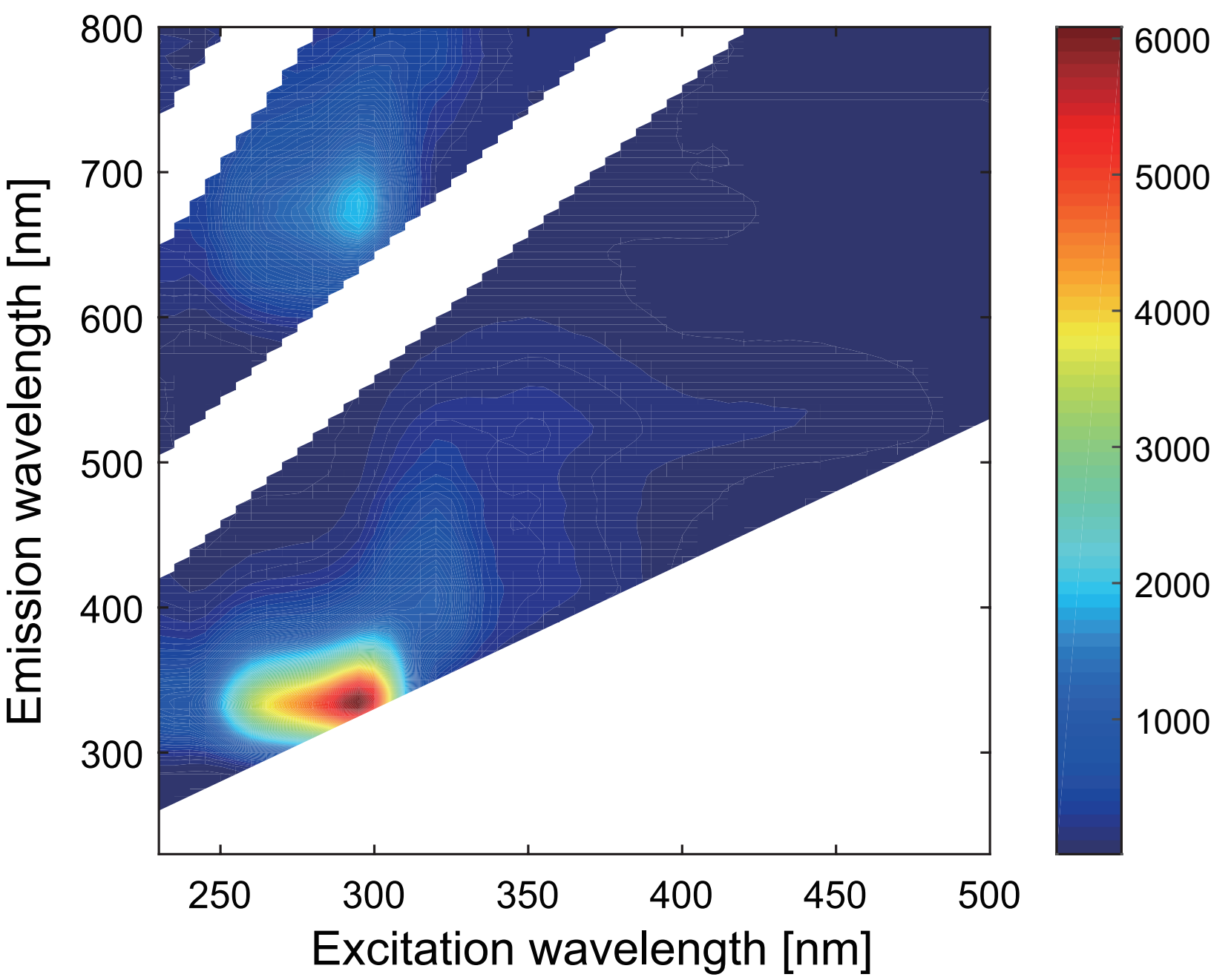
**Table 2**

Results of PLS regression for four pretreatment methods.

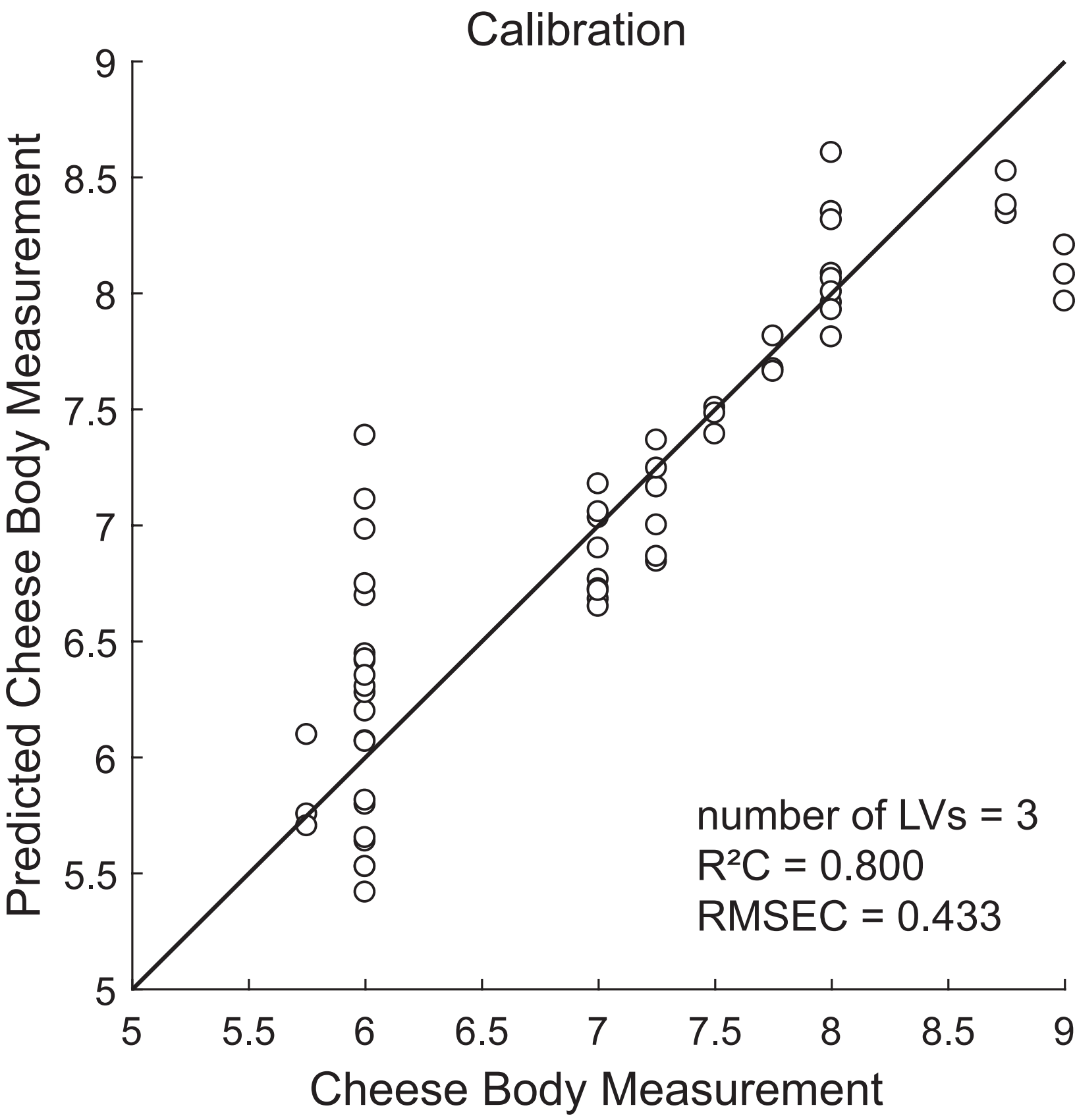
Pretreatment	LVs	RMSECV	R <sup>2</sup> CV	R <sup>2</sup> C *	R <sup>2</sup> P	RMCEP
mean center	3	0.456	0.787	0.800	0.826	0.436
normalize + mean center	3	0.456	0.787	0.808	0.747	0.515
autoscale	3	0.493	0.757	0.822	0.787	0.470
normalize + autoscale	2	0.482	0.762	0.787	0.739	0.519

\* The coefficients of determination for calibration.

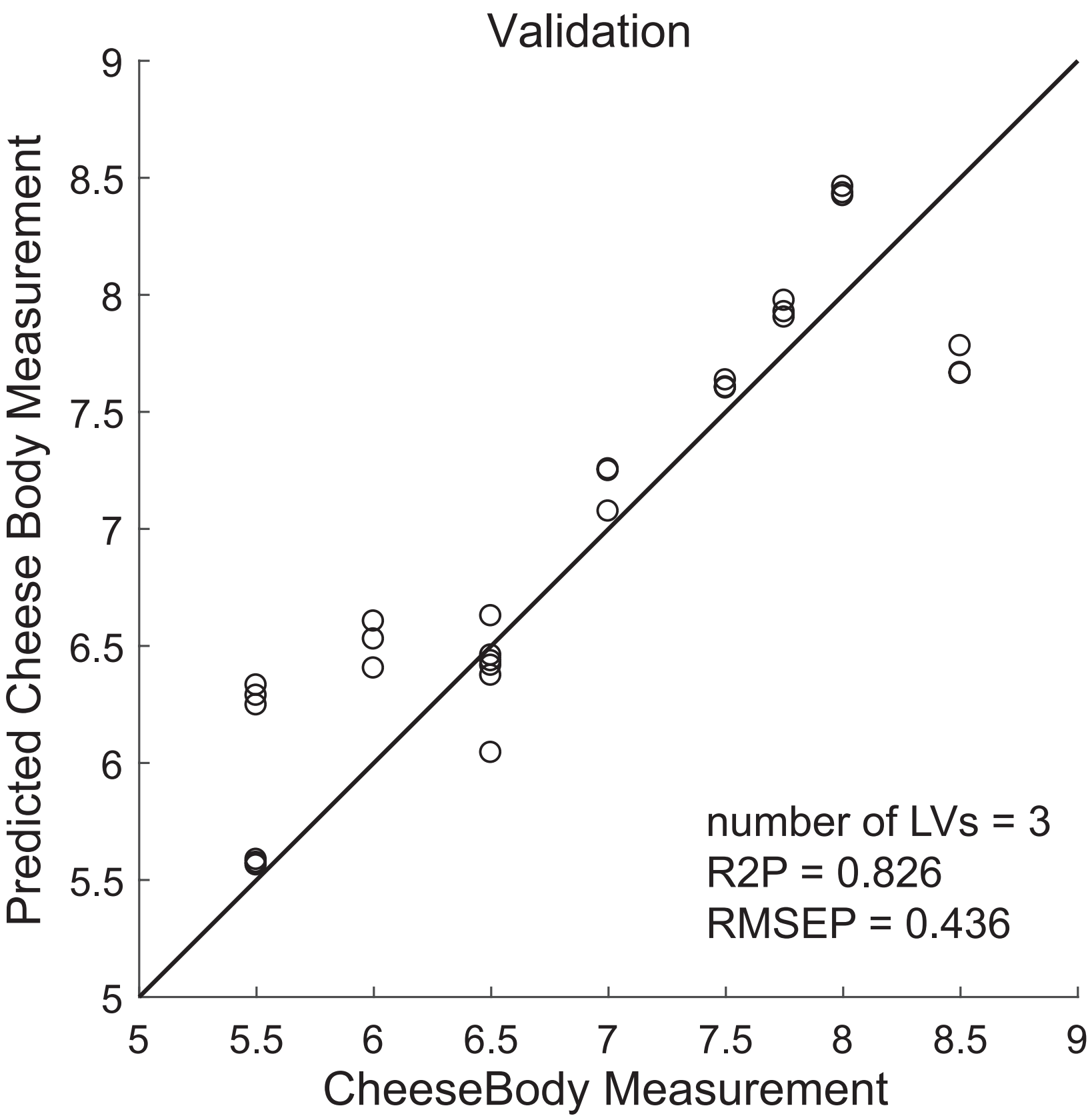
Figure



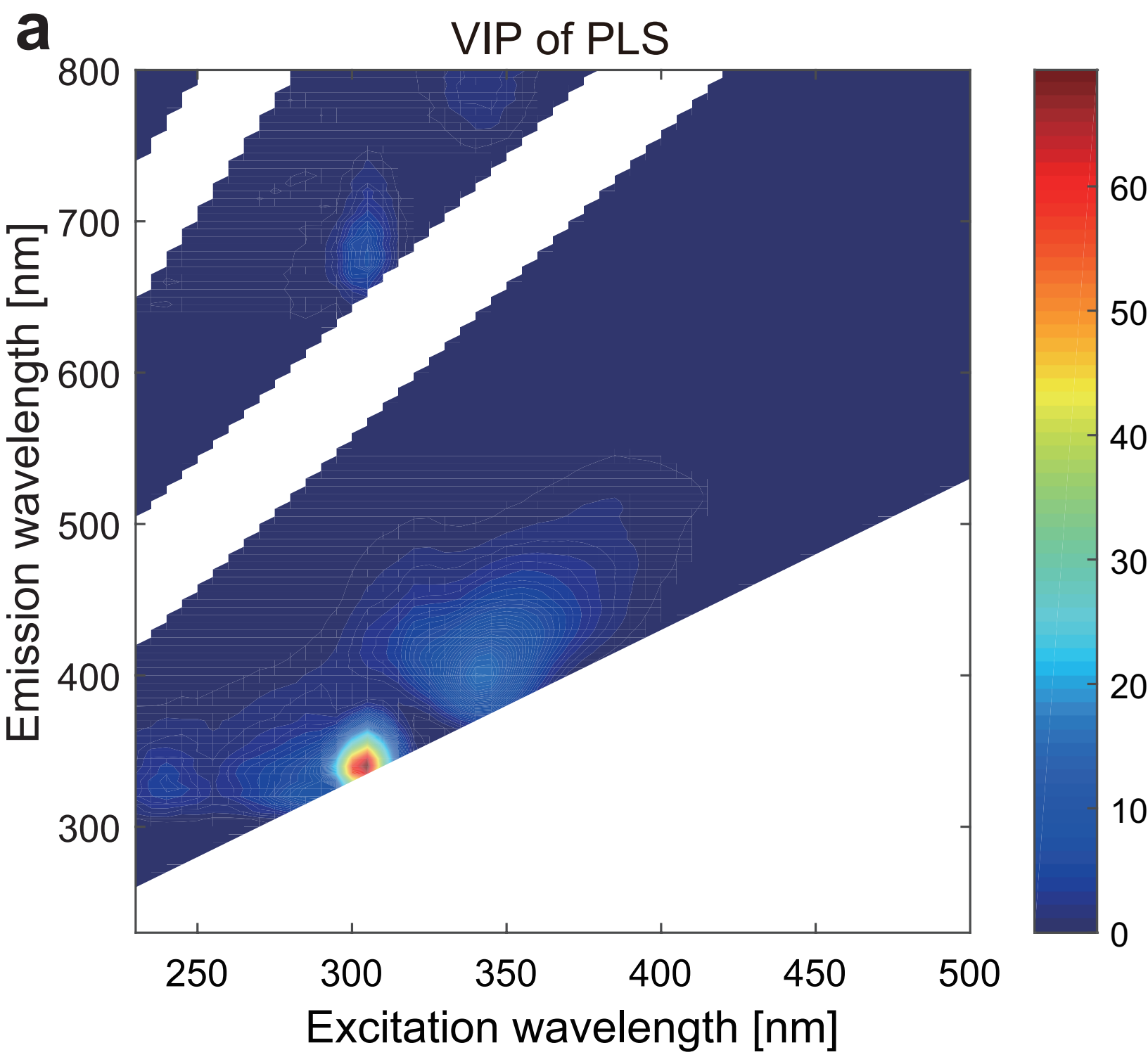
Figure

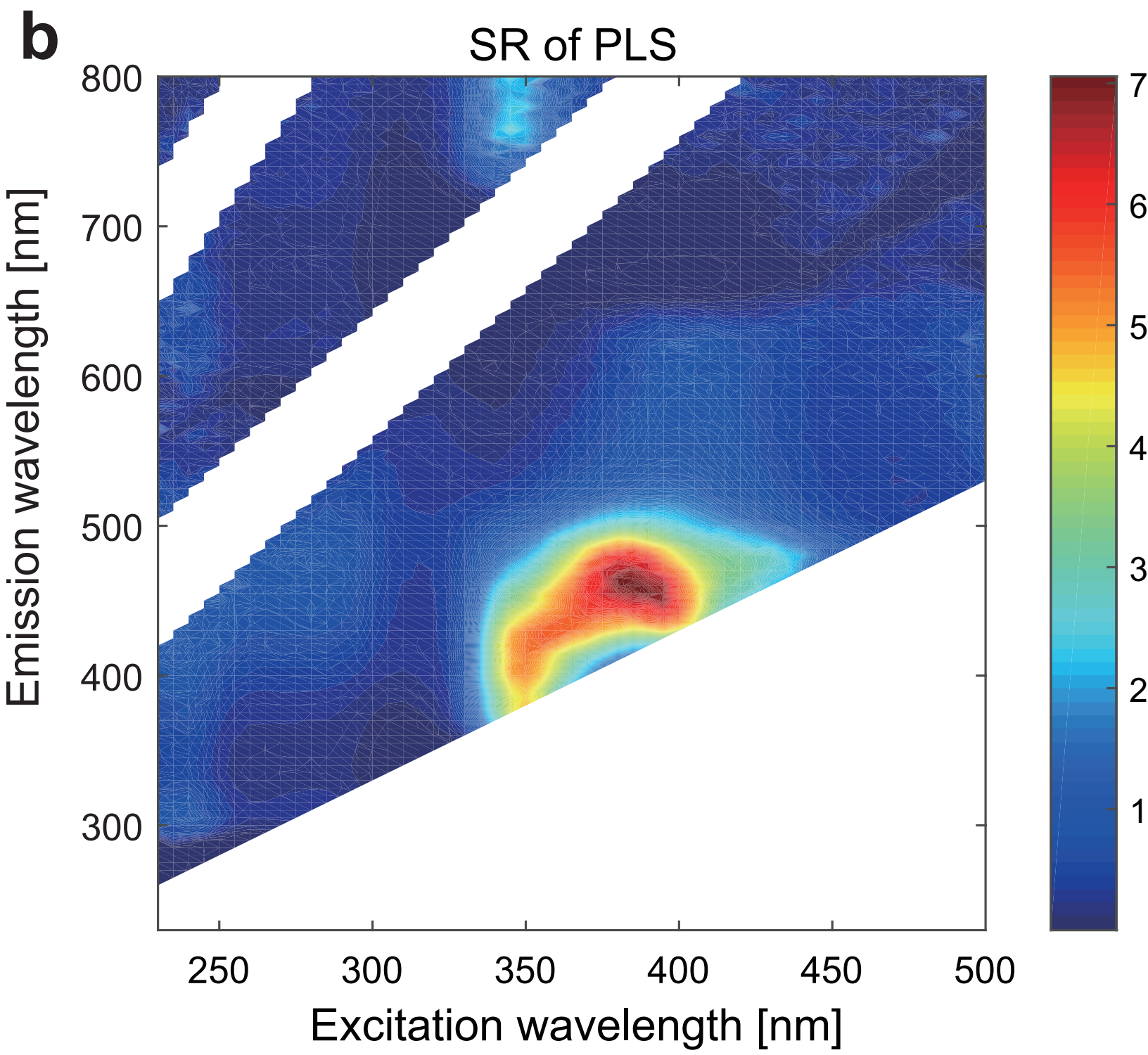


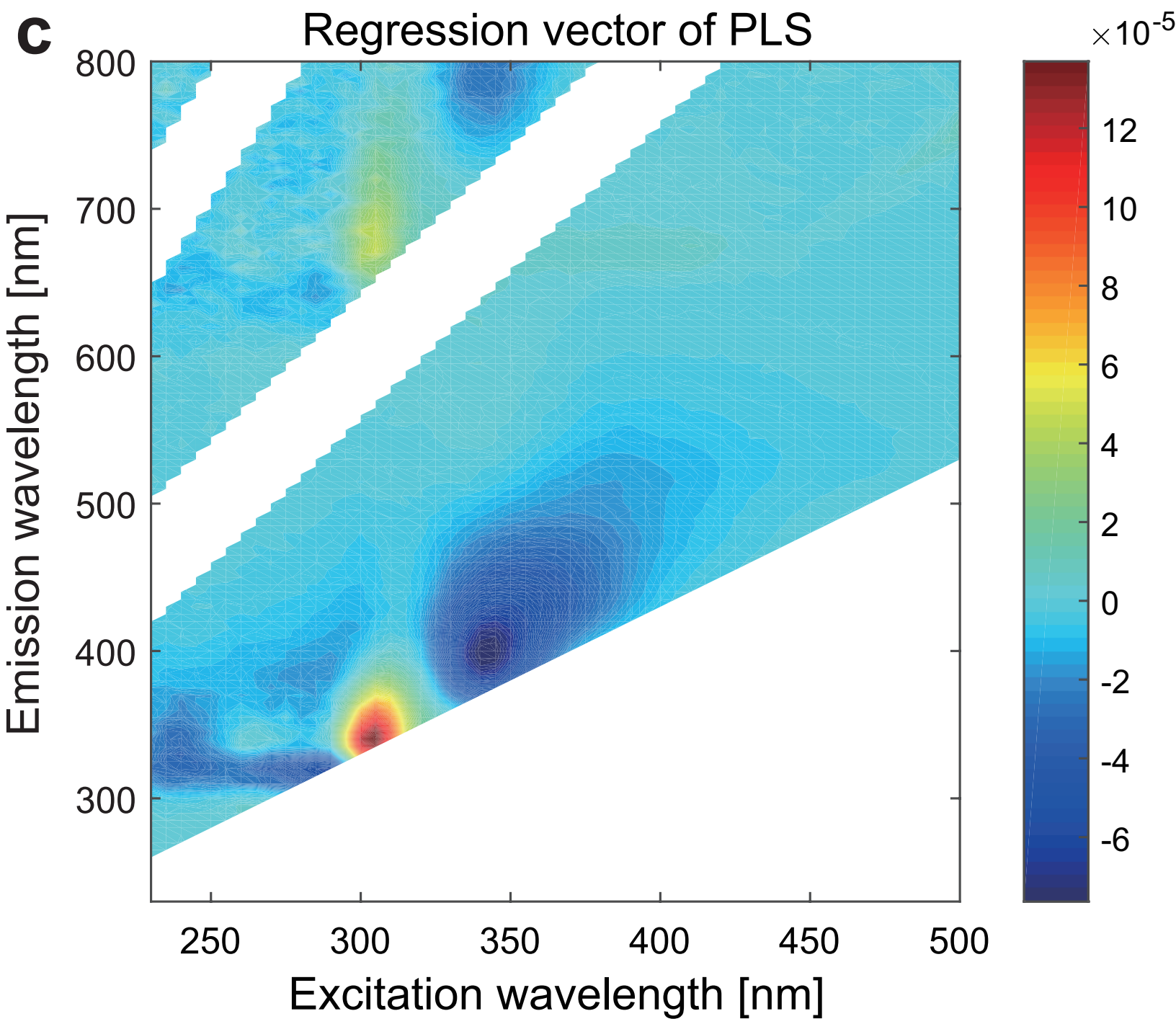
Figure



Figure

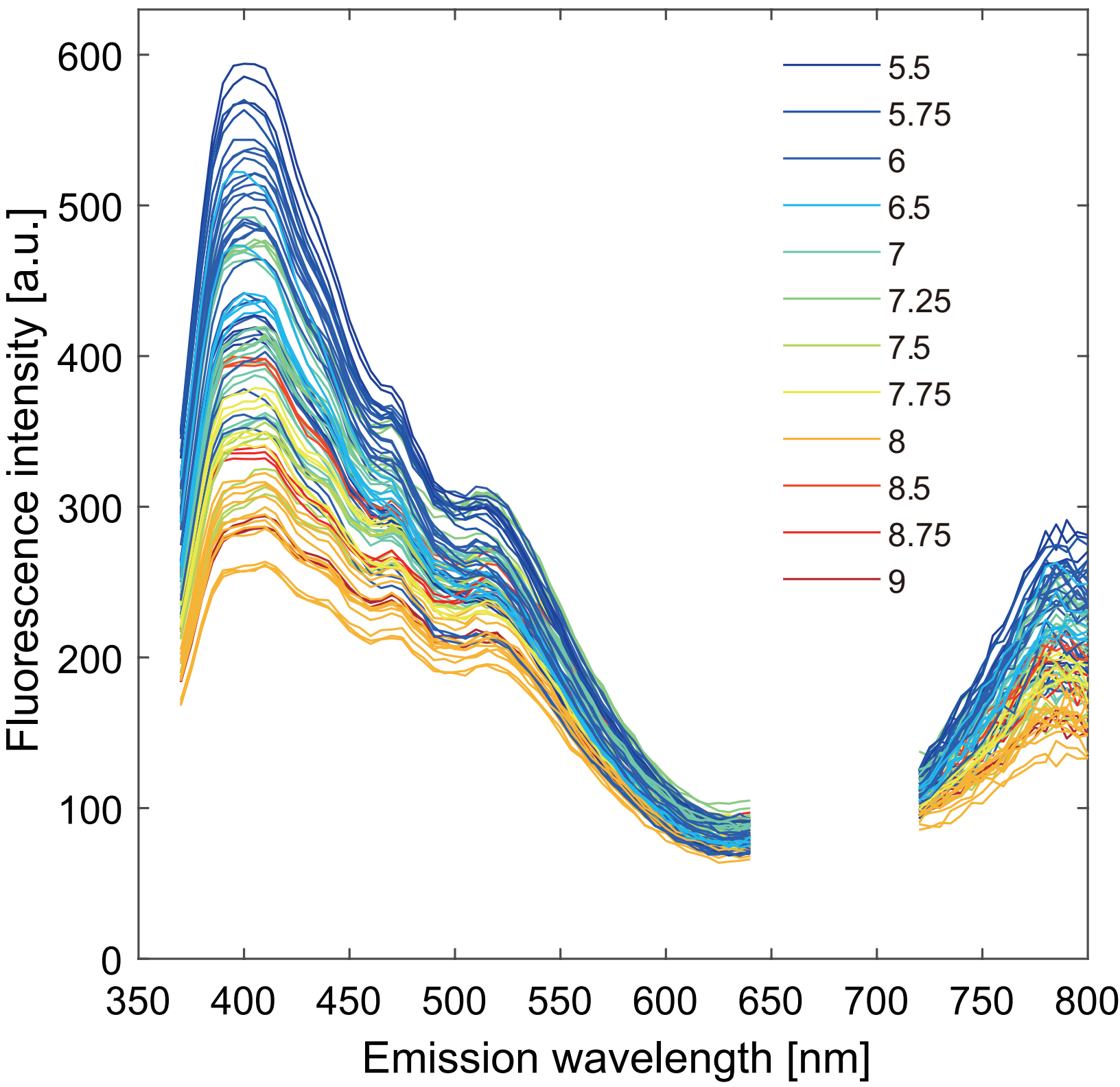




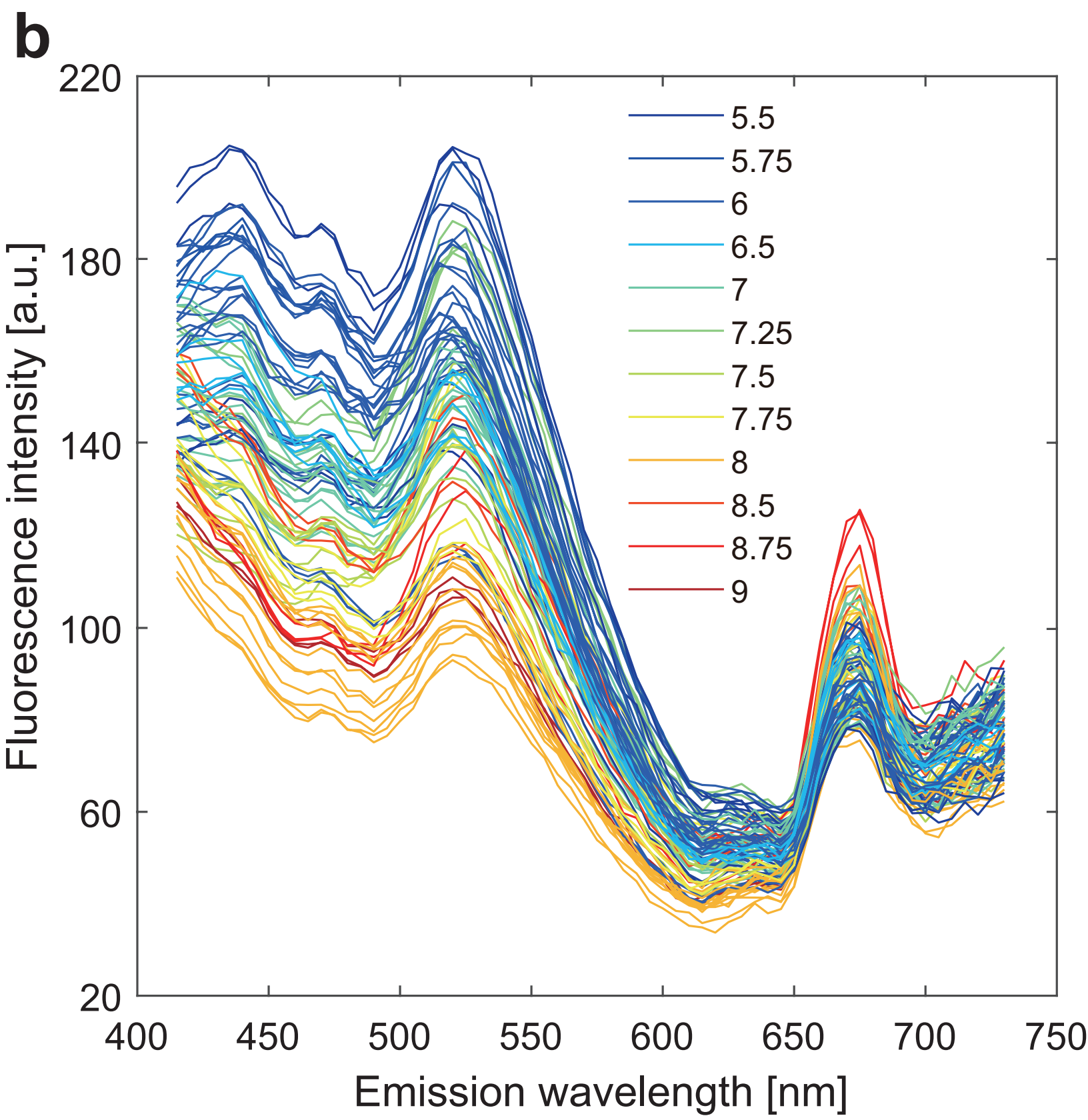


Figure

**a**



Figure



Figure

**c**

